# Two-phase deformation of lower mantle mineral analogs


Pamela Kaercher[1], Lowell Miyagi[2], Waruntorn Kanitpanyacharoen[1], Eloisa Zepeda-Alarcon[1], Yangbin Wang[3], Francesco De Carlo[3], Hans-Rudolph Wenk[1]

[1]Department of Earth and Planetary Science, University of California, Berkeley, CA · [2]Department of Geology and Geophysics, The University of Utah, Salt Lake City, UT · [3]Advanced Photon Source, Argonne National Laboratory, Argonne, Illinois


## Introduction

While much is known about preferred orientation in single phase aggregates, deformation of polyphase materials is still enigmatic. Most of the Earth is composed of polymineralic rocks, including the lower mantle which is of critical importance for understanding the geodynamic evolution of the planet. Of the few studies which have examined deformation in mantle mineral composites (e.g. Li et al. 2007), none have examined lattice preferred orientation.

$(Mg,Fe)_2SiO_4$ (Olivine) → $(Mg,Fe)_2SiO_4$ (Wadsleyite) → $(Mg,Fe)_2SiO_4$ (Ringwoodite) → $(Mg,Fe)O$ + $(Mg,Fe)SiO_3$ (Ferropericlase + Mg-perovskite)

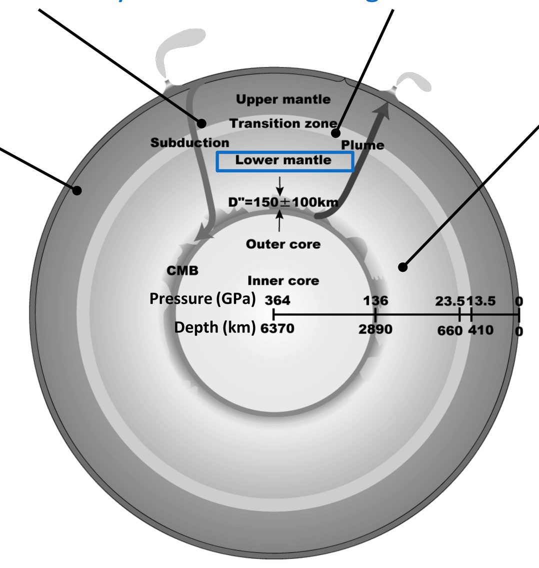


The lower mantle is composed primarily of two mineral phases:

**Mg-perovskite**

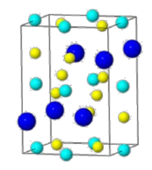


Stiff
K = 246 GPa

**Ferropericlase**

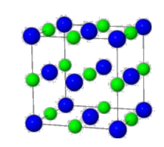


Weak
K = 160 GPa

During deformation, is the minor, weak phase isolated in pockets and grain boundary junctions so that the bulk deformation has to occur in the hard phase? Or does the soft phase lubricate grain boundaries so that it concentrates deformation, and the hard phase moves as rigid blocks?

## D-DIA

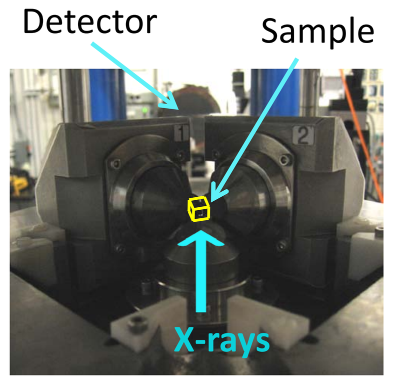


Samples were deformed in the D-DIA at APS. Sintered cylinders of various volume fractions of the two phases were compressed then stressed uniaxially. Diffraction patterns were collected *in situ* up to approximately 4 GPa, 800°C , and 50% strain in order to observe evolution of preferred orientation.

## Analog Minerals

**Neighborite ($NaMgF_3$)**

1. Isostructural to $(Mg,Fe)SiO_3$
2. $K_{NaMgF_3} \approx \frac{1}{3} K_{(Mg,Fe)SiO_3}$
3. Possible slip systems of $(Mg,Fe)SiO_3$ : (001),(010)[100],(100) [010] of $NaMgF_3$ : {1-10}<110>, (001)<100>

**Halite (NaCl)**

1. Isostructural to (Mg,Fe)O
2. $K_{NaCl} \approx \frac{1}{6} K_{(Mg,Fe)O}$
3. Same slip systems as (Mg,Fe)O: {110}<1-10>, {111}<1-10>, {100}<1-10>

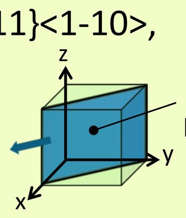


Since lower mantle conditions are beyond the capabilities of D-DIA, we used neighborite ($NaMgF_3$) as the hard phase analog of magnesium-silicate perovskite (Zhao et al. 1993; Liu et al. 2005) and halite (NaCl) as the soft phase analog of ferropericlase.

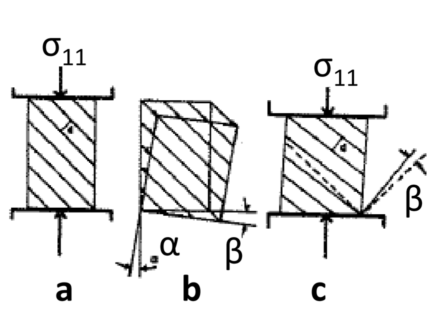


**Lattice rotation leads to lattice preferred orientation and seismic anisotropy**

Solid lines are slip planes. (a) uniaxial stress is applied causing (b) shear deformation. (c) slip plane normal rotates toward the compression direction.

## Microtomography

Microtomography of one undeformed and two deformed samples was performed at beamline 2-BM of the APS. Raw images where processed first in Octopus software to produce orthoslices, then in Avizo Fire to create 2D and 3D rendering of the sample and grain statistics which are shown below.

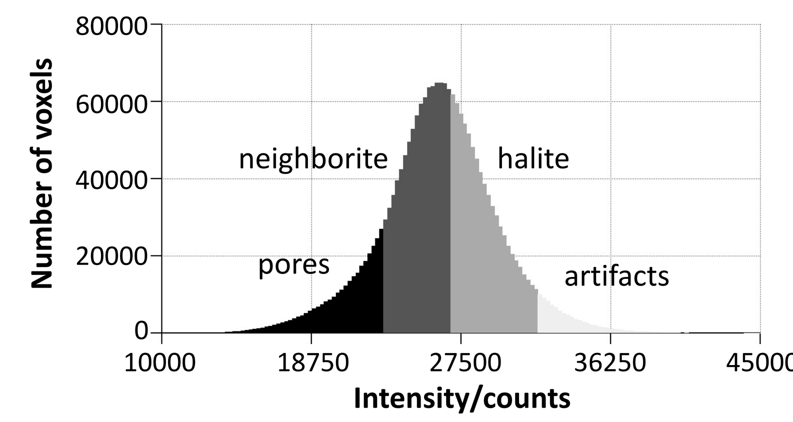


Halite grains were a slightly lighter shade of gray due to having a slightly higher atomic number than neighborite and thus greater absorption.

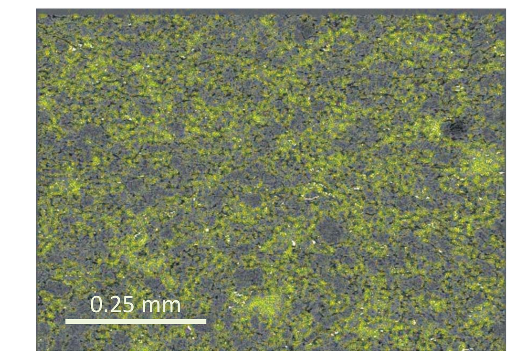


Halite grains (shown in green) surround the neighborite grains (gray).

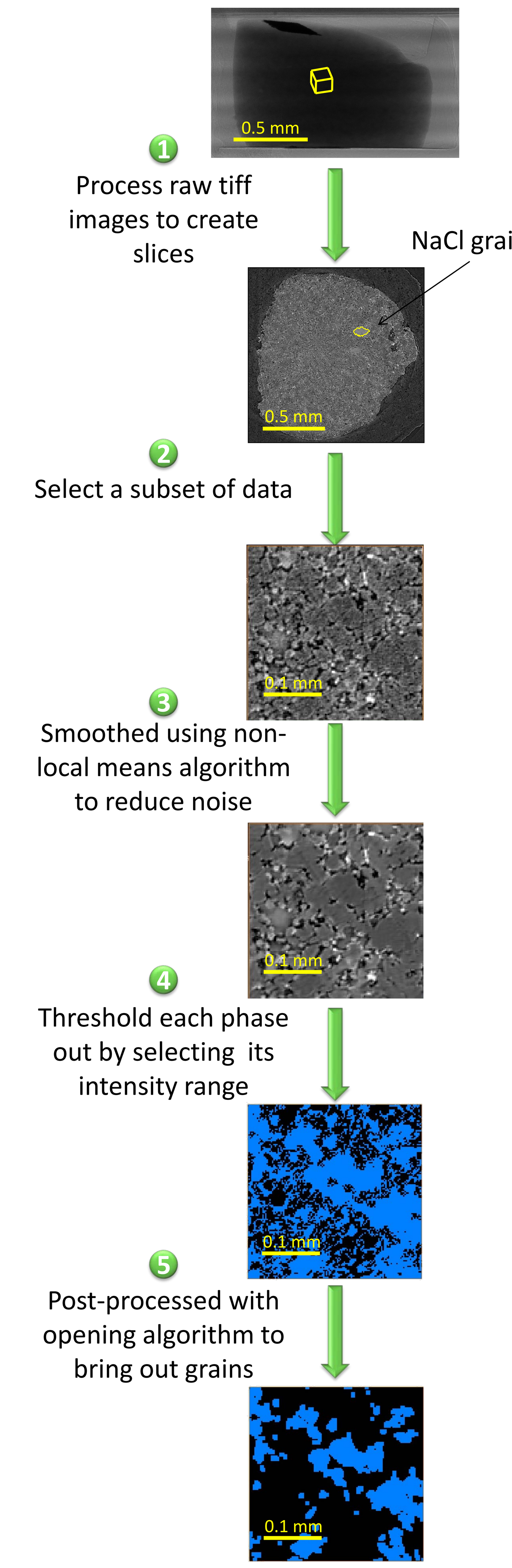


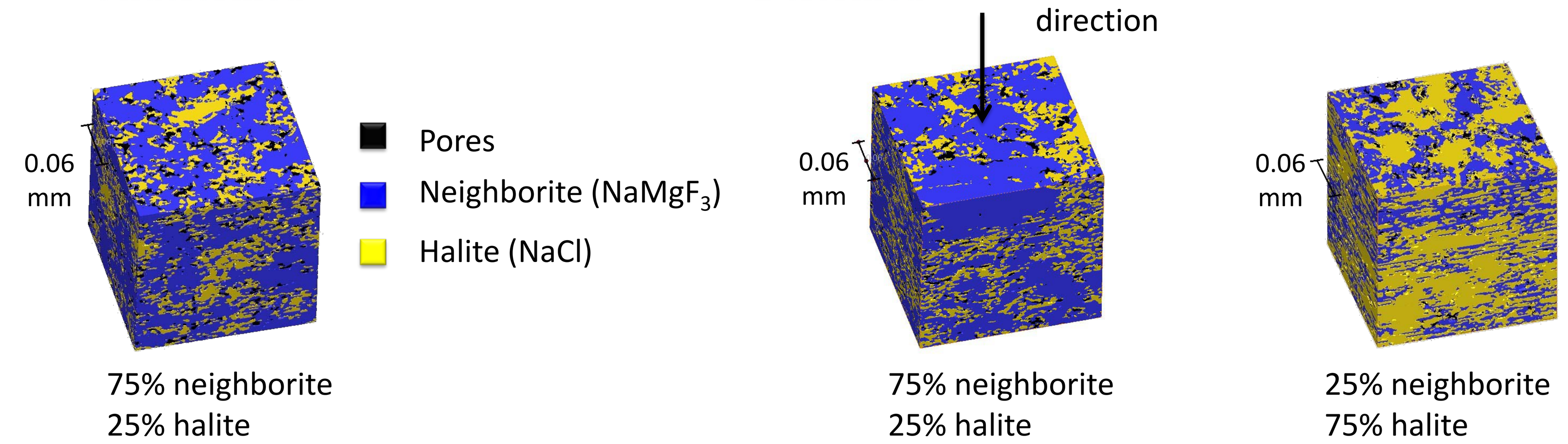



Orthoslices in the XZ plane showing initial and deformed grains .

Histograms showing aspect ratios for neighborite and halite grains. There are a greater number of grains with an aspect ratio ≈1 in the undeformed sample, but a great number of grains with larger aspect ratios in the deformed samples.

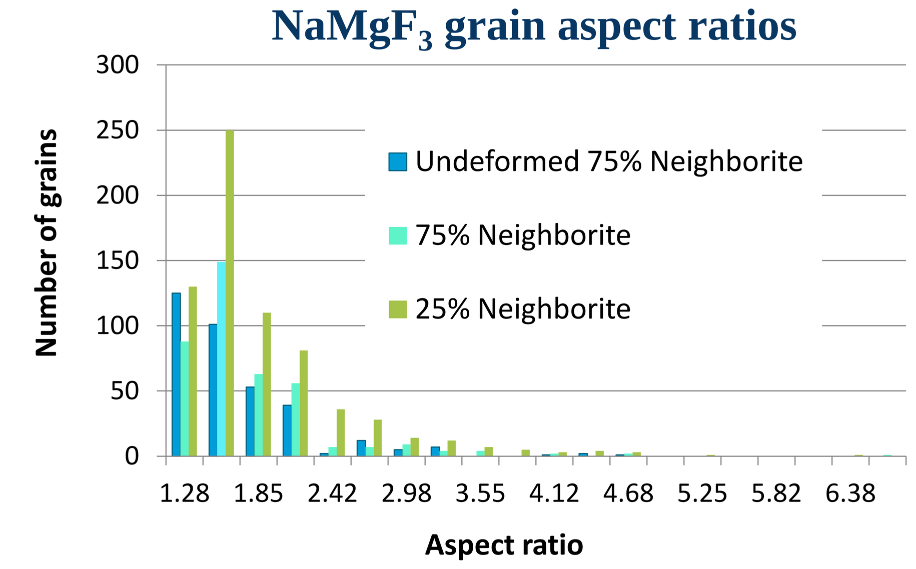


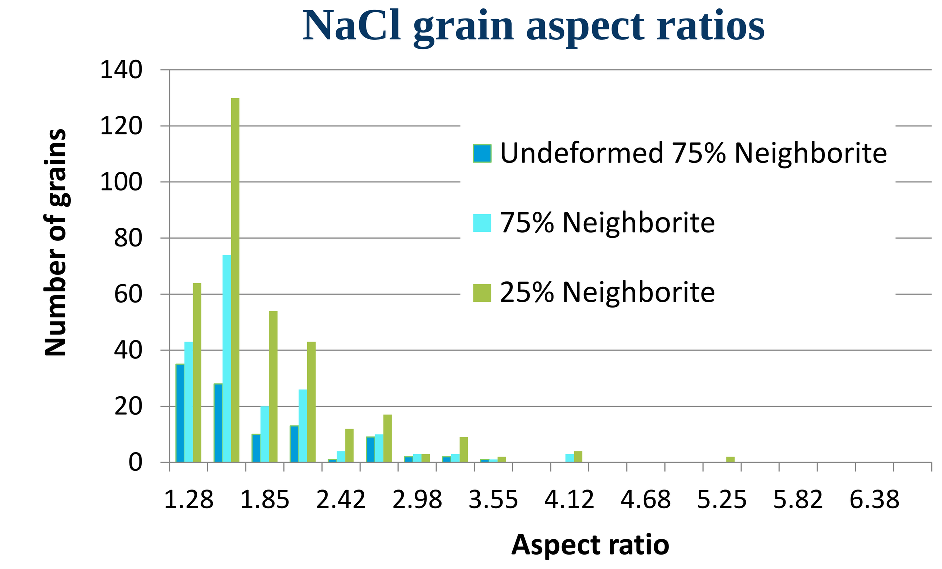


Unrolled spectrum for 75% $NaMgF_3$ + 25% NaCl
Dotted blue line is collected data. Solid black line is calculated fit.

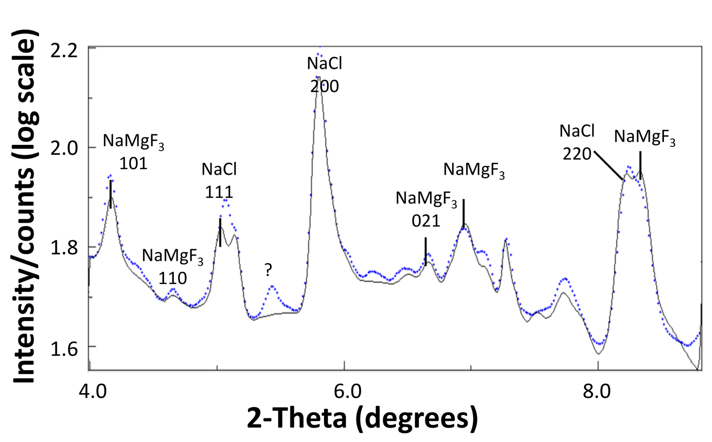


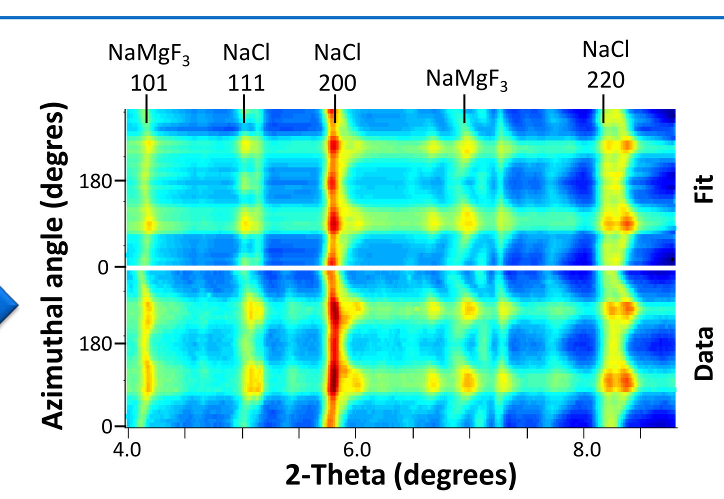


2D plot for 75% $NaMgF_3$ + 25% NaCl. Curviness of lines shows degree of elastic strain. Halite curves are straighter suggesting that it absorbs the deformation. Change in intensity with azimuthal angle denotes plastic strain resulting in lattice preferred orientation.

The Rietveld method as implemented in the software package MAUD was applied to identify phases and quantify preferred orientation.
Initial results from D-DIA experiments show that texture strength in neighborite increases with decreasing halite content. This suggests that the softer phase, NaCl, absorbs much of the deformation. Interestingly texture of halite is very weak as if hard particles enforce strain shadows and cause local heterogeneity.

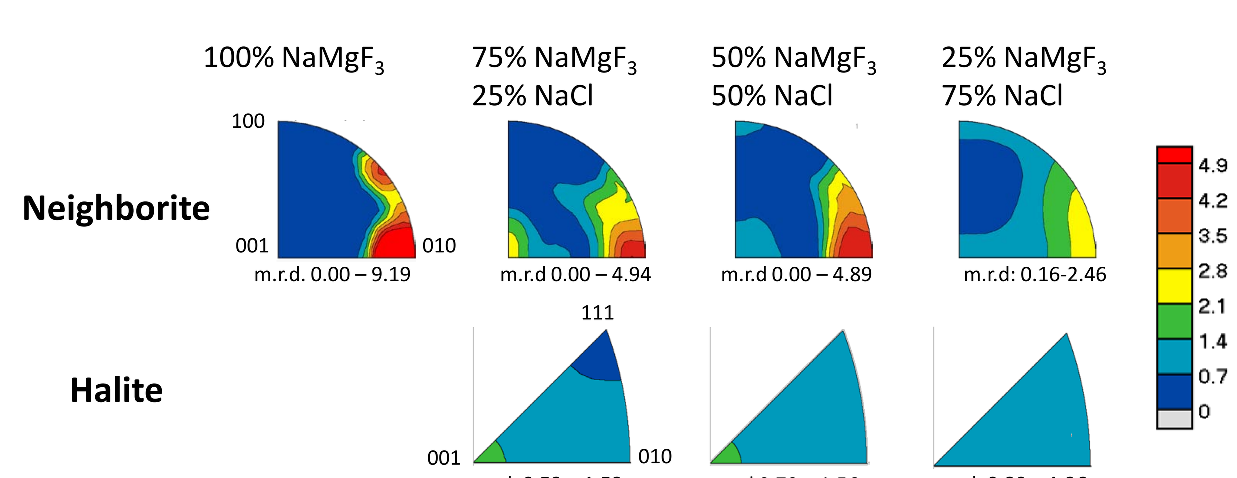


Inverse pole figures for neighborite-halite mixtures compressed to 3 GPa, deformed to 15% strain and heated to 400 °C in D-DIA, illustrating the effect of volume fractions on texture strength.

## Conclusion

Initial results from D-DIA experiments show that texture strength in neighborite increases with decreasing halite content. This suggests that the softer phase, NaCl, absorbs much of the deformation. Interestingly texture of halite is very weak as if hard particles enforce strain shadows and cause local heterogeneity. Microtomography data collected at beamline 2-BM at the APS supports this. Processed tomography data for a deformed sample of 75% $NaMgF_3$ + 25% NaCl shows that soft halite surrounds the harder grains of neighborite. These preliminary findings are very encouraging and experiments, both on texture and microstructure are being continued. Further experiments and FEM modeling (Quey et al. 2011) will be done in order to accurately quantify the contribution of each mineral phase to the final texture of the composite. These results can then be input into models of the lower mantle (e.g. Wenk et al. 2011) to improve our understanding Earth's geodynamics.


## Acknowledgements

We thank CDAC for financial support and APS for the use of beamlines 13-BM-D and 2-BM-XOR.


## References


Li L, Addad A, Weidner D, Long H, Chen J (2007). Tectonophysics 439:107-117.
Liu HZ, Chen J, Hu J, Martin CD, Weidner DJ, Hausermann D, Mao HK (2005). Geophy. Res. Lett. 32, doi: 10.1029/2004GL022068.
Quey R, Dawson P, Barbe F (2011). Comput. Methods Appl. Mech. Engrg., 200:1729-1745.
Wenk HR, Cottaar S, Tomé C, McNamara A, Romanowicz B (2011). EPSL-10860.
Zhao Y, Weidner DJ, Parise JB, Cox DE (1993). PartI. Phys. Earth Planet. Inter., 76:1-16.